Optimisation of the Serration Outline Shape of a Single Offset-Fed Compact Antenna Test Range Reflector Using A Genetic Evolution of the Superformula

Marc Dirix[1], Stuart F. Gregson[2,3]
[1] Antenna Systems Solutions, Santander, Spain, mdirix@asysol.com
[2] Next Phase Measurements LLC, USA, stuart.gregson@npmeas.com
[3] Queen Mary University of London, London, UK, stuart.gregson@qmul.ac.uk

***Abstract*—While the size of the reflector in general determines the usable area of the quiet zone inside which plane wave conditions are found, the edge treatment also plays a significant role in terms of overall quality and electromagnetic field distribution. Using modern fast simulation technology in combination with genetic optimisation, the edge treatment can be optimised specifically for a compact antenna test range as part of the design process. This is crucial as it maximises the efficiency with which the available space is used and therefore minimises the costs of implementation of a new facility. This is particularly important in 5G applications where multiple systems are typically required with any economies becoming multiplicative. Several commonly encountered reflector edge treatments are examined with the quiet-zone performances compared against that of an alternative genetically optimised serration design.**

***Index Terms*—CATR, antenna measurement, serrations, genetic optimization, 5G**

I. INTRODUCTION

Single offset reflector compact antenna test ranges (CATRs) are a well-known solution for taking far-field (FF) measurements in limited spaces. A parabolically shaped reflector is used as collimator of the quasi-spherically diverging electromagnetic field radiated by an electrically small feed antenna and transforms it into a pseudo plane-wave within a limited region of space that is situated in front of the reflector. The coupling of this quasi-plane-wave into the aperture field of the antenna under test (AUT) produces the classical "far-field" measured antenna radiation pattern. Clearly then, the accuracy of a pattern measurement taken in this type of measurement range is predominantly determined by the quality of the pseudo plane-wave. The amplitude and phase uniformity of this pseudo plane-wave is determined principally by two factors, the amplitude- and phase-taper (which is largely governed by the radiation pattern function of the CATR feed antenna and its location with respect to the reflecting surface), and high spatial frequency ripple determined by the properties of the diffracted field originating from the reflector edge treatment [1]. This collimating effect is inherently broadband. However, the upper frequency limit depends largely on the reflector surface accuracy, with installed systems covering the mm-wave and sub mm-wave bands [1]. Conversely, the lower frequency limit is governed by the finite size of the reflector, the reflector edge treatment, and the wavelength of the illuminating radiation. Together these factors determine the cross-sectional area of the pseudo-plane-wave with the region of space throughout which the collimated field approximates a true TEM plane-wave determining the size of the CATR quiet-zone (QZ).

Since the reflector edge treatment is of such importance to the performance of the CATR, several types of termination have been proposed, with the most commonly implemented being the serrated edge, *i.e.* castellated, design as proposed by E.B. Joy [2], [3] and [4], and the blended rolled edge design [5], [6] and [7] which was devised by W.D. Burnside. The serrated edge treatment can be conceived as being a way to provide a smooth tapering, *i.e.* windowing, of the reflected field thereby providing a smooth transition from the low surface impedance of the reflector body, to the 377 Ω impedance of free-space elsewhere. Previously, the design of the serration shape has received some considerable attention in the open literature [8], [9] [10], [11] and [12] where research has largely concluded that, for many applications, the $\cos^2$ or an engineering compromise thereof, and circular-segmented shape provide the best performance.

In this paper an alternative approach is adopted. The novel approach used herein employs the Superformula [13] to specify the shape outline of the individual serrations. This method has the inherent advantage that by varying a relatively limited number of input parameters, the edge shape of the serrations can be greatly varied, allowing for example, the shape to be adjusted from convex to concave form permitting a large variety of shapes in between. The utilisation of the Superformula and its use in shaping the CATR serrations will be discussed in more detail in Section II below. The optimisation of the edge shape of the serrations is thus found by variation of the input parameters to the Superformula using a Darwinian evolution principle [14] based genetic evolution algorithm [15]. Details of the genetic optimisation (GO)

algorithm are presented below within Section III. Section IV contains the CATR QZ results with Section V presenting the summary and conclusions from this study.

II. SERRATION SHAPE

In this section we concentrate on specifying and controlling the CATR serration shape, whilst paying particular attention to its definition using the Superformula.

A. Serration Shape Outline

The shape of the CATR serrations have received attention from several workers with several designs being investigated with the most widely examined including linear, *i.e.* triangular, and cosine shaped serration being perhaps the predominant choice for the shape. In [8] it was shown that the circular shaped serrations can provide a further improvement over the linear and cosine shape developed in [2]. Here, cosine shaped serrations are described by:

$$w(l) = \pm 0.5 w_0 \cos^A\left(\frac{\pi}{2l_0} l\right) \tag{1}$$

where w_0, l_0 are the width and length of the single serration respectively, and A is the cosine exponent, with typically $A = 1.6$ however this may be varied to find optimal performance for a given range. Conversely, circular shaped serrations can be obtained using:

$$\begin{aligned} w(l) &= \pm\left(\sqrt{r^2 - l^2}\right) + \frac{1}{2}w_0 - r \qquad 0 \le l \le \frac{1}{2}l_0 \\ w(l) &= \mp\left(\sqrt{r^2 - (l_0 - l)^2}\right) + r \qquad \frac{1}{2}l_0 \le l \le l_0 \end{aligned} \tag{2}$$

with,

$$r = \frac{1}{8}w_0 + \frac{1}{2}\frac{l_0^2}{w_0} \tag{3}$$

As can be seen from Eqns. (2) and (3), the circular shaped outline does not allow for any further optimization in terms of the profile of the shape , with only a variation of the width and length being permissible. The resulting serration shapes for the cosine and circular functions are shown in Figure 1 below.

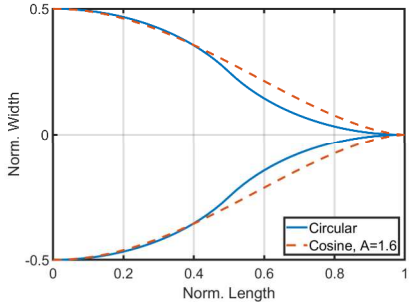

Figure 1:Normalized circular and cosine (A=1.6) shaped serrations.

The Superformula [13] is a generalisation of the Lamé curve (superellipse) and can be used to described a multitude of circular symmetric two-dimensional shapes that are commonly found in nature. The Superformula when expressed in polar form can be expressed as:

$$r(\varphi) = \left(\left|\frac{1}{a}\cos\left(\frac{m}{4}\varphi\right)\right|^{n_2} + \left|\frac{1}{b}\cos\left(\frac{m}{4}\varphi\right)\right|^{n_3}\right)^{-\frac{1}{n_1}} \tag{4}$$

where m describes the number of rotational symmetries, a, b are amplitude factors and n_1, n_2 and n_3 determine the radial shape. The resulting shape can then be transformed to cartesian coordinates using:

$$C(x, y) = r(\varphi)\cos\varphi\,\hat{x} + r(\varphi)\sin\varphi\,\hat{y} \tag{5}$$

Thus, depending on the rotational symmetry, monogons ($m = 1$), diagons ($m = 2$) and polygons ($m > 2$) can be formed. Given the shape of the serrations, *e.g.* a symmetric, centred "spike" of certain shape with a broad flat base, monogons and diagons are the only forms of interest for this research. Moreover, only the first and fourth quadrant are of interest for the shape of the serration. As a result, in order to determine the shape of the serration the parameter variation of the Superformula can be limit to $m = 2$, because the diagon is better behaved than the monogon due to its symmetry at the y-axis. To further limit the search space, and making sure the final shape is continuous, the following parameter limitations are applied:

$$\begin{aligned} n_2 &\le n_1 \\ n_3 &= n_2 \end{aligned} \tag{6}$$

Using these parameter limitations, the serration shape can be continuously varied between a convex, linear, cosine and circular shape. In Figure 2, a few possible serration shape outlines are illustrated for various values of the input parameters n_1, n_2 and n_3.

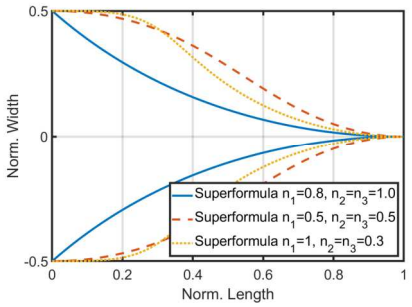

Figure 2:Normalized Superformula shaped serrations.

While the optimization, as will be detailed in section IV, is currently limited to a single frequency, due to the nature of the serrations shapes found with the Superformula, it is expected that the results remain as broadband as the cosine and circular-segmented shapes.

B. Serration base widths and relative angle

With the described formulation in Section A the shape outline of each serration is defined. However, the ripple in the QZ can further be reduced by preventing any coherence in the scattered wave from the edges of the serrations by varying the widths of the serration base and the relative angle

at which they emanate from the reflector main, *i.e.* solid, body. Thus, to be able to limit the number of parameters that need to be optimised, the inherent symmetry provided by a quadratic reflector is used. This can clearly be easily expanded to consider rectangular reflector configurations. With the main symmetry axis being a horizontal and vertical cut through the centre of the reflector, the serrations can be divided into 8 sections. Each of these sections then uses the same variation of width and angle for the individual serrations within its section starting from the symmetry line, running out to the reflector cross-directed boundary. To further reduce the number of parameters, the widths and angles are described using a quadratic function of a single variable. Here, the function is created such that for the widths at the lower boundary, all serrations have equal widths. Conversely, the upper boundary width of the serrations increases quadratically while keeping the inner serrations at a practical minimum size.

Similarly, a corresponding function is devised to determine the angle relative to the symmetry axis, with the tilt angle ranging from 0° (straight) out, to 45° for the corner serration. In Figure 3 the maximum variation of the widths and angles of each serration starting from the symmetry line is shown using a cosine outline.

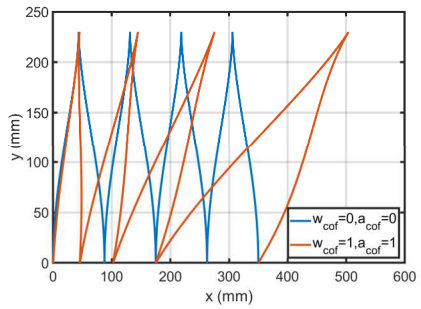

Figure 3:Variation of serration widths and angles by width- and angle coefficient.

III. Quiet Zone Simulation

A. Simulation using GO algorithm.

For anything other than the simplest of configurations, it is typically very difficult to derive closed form analytical solutions for the electromagnetic field at a given point in space from electric and/or magnetic fields specified across a known, curved, surface. As such, recourse to typically numerical based modelling techniques becomes necessary. It is possible to simulate a CATR using a full-wave three-dimensional CEM solver. And this approach would have the advantage of, arguably, introducing the smallest number of assumptions and approximations. However, at the time of writing, although many solvers are available, these are largely considered inappropriate for simulating problem spaces as electrically large as those needed to enclose a complete high frequency CATR system when the intent is to place the solver within an intensive optimization loop. Fortunately, we may fall back on physical optics (PO) based modelling techniques which can, when deployed in an appropriate way, provide the requisite accuracy and efficiency. Thus, in this study, the current elements method was harnessed [1]. Here, we replace the fields radiated by the feed with an equivalent surface current density $\underline{J_s}$ which can subsequently be used as an equivalent source to the original fields. Then, the magnetic and electric fields radiated by an electric current element can be obtained from the free-space Green's function and the vector potential [1]. Integrating this impressed current across the reflector surface thereby allows the computation of the CATR quiet zone (QZ).

The efficiency of the computation can be further improved by noting that the illumination of the reflector may be evaluated once, prior to entering the optimisation loop, with only the field propagation from the reflector surface to the CATR QZ requiring evaluation within the optimisation loop. A further powerful feature of this approach is that the field propagation itself is embarrassingly parallelable. Although in practice there is some overhead associated with breaking the problem up and distributing it to an ensemble of individual processors with more effort being required to aggregate the complete CATR QZ field once computed, for the case of modern digital computers comprising typically 8 to 64 individual CPUs, this makes the field propagation calculation complete in much less than a second. This is true for many 5G mm-wave CATRs intended for Massive MIMO test applications. Clearly then, such an approach enables the designer to run tests comprising tens of thousands of simulations in a matter of only a few hours and it is this huge efficiency that underpins the successful use of genetic optimisation.

B. Genetic optimization

Due to the comparatively wide number of parameters that are required to be optimized simultaneously, neither a linear parameter sweep, nor a fully random optimization strategy were found to be able to converge sufficiently quickly to enable the optimum solution to be determined. Therefore, a genetic algorithm was employed that was the analogue of the algorithm presented in [15]. The genetic algorithm utilized herein can be seen presented in *Figure 4* below. Here, an initial population was generated using a randomized set of initial parameters so as to produce a wide spread of the design parameters. After simulation, the fitness value of each individual was determined. The population was then pruned, and parents of the next generation were selected. These parents were then used to produce new children, *i.e.* individuals, by means of parameter cross-over and mutations (which were implemented through random changes of the underlying genes).

```
Begin
   INITALIZE POPULATION
   REPEAT UNTIL (TERMINATION CONDITION) DO
      EVALUATE NEW CANDIDATES
      PRUNE POPULATION
      CREATE OFFSPRING
   END DO
END
```

Figure 4: The genetic algorithm in pseudocode

The fitness value, *i.e.* penalty function, used was based on an assessment of the ideal QZ field which was assumed to comprise a plane-wave which has constant amplitude and phase in any direction perpendicular to the wave propagation. The fitness value was then computed from the sum of both the standard deviation of the amplitude and the standard deviation of the phase. It was found that this "summed" fitness value places equal significance on the uniformity of the amplitude and phase functions. Furthermore, the variation of the fitness value as a function of generation was used to establish a termination condition. When an optimum solution is found in terms of parameter configuration, the variation of the fitness value output between iterations will remain below a certain predetermined threshold, and thus allows the algorithm to terminate

IV. Simulation Results

To illustrate the applicability of the CATR optimization algorithm, an existing CATR designed for 5G applications was chosen as a starting point. The CATR comprised a corner offset fed reflector that was conceived to provide a 600 mm diameter, cylindrically shaped QZ, with its main operational frequencies residing in the 5G FR2 mm-wave band. The genetic algorithm as described above was then utilized to simultaneously optimize the outline shape of the serrations, together with the angle- and widths-functions. The optimization was evaluated at a single frequency, which in this case was 18 GHz, after which the optimized shaped reflector was further simulated at 12.4 and 26.5 GHz to verify the resulting design was broadband. The final results were then compared to the cosine shape Eqn. (1), and the circular-segmented Eqn. (2) where each of these had fixed angles from the corner to the symmetry line [30, 0, 0, 0] (deg) and widths from the corner to the symmetry line [20 10 10 10] (%) which were selected as being representative of values that have been used successfully in other applications.

	Cosine$^{1.6}$			Circular-segmented			Genetic Optimized		
f	12.4	18.0	26.5	12.4	18.0	26.5	12.4	18.0	26.5
A_v	0.81	0.93	0.92	1.29	1.05	0.94	0.93	0.66	0.78
A_t	0.45	0.91	0.80	0.85	0.83	0.80	0.63	0.62	0.80
A_r	0.34	0.19	0.23	0.49	0.38	0.28	0.27	0.21	0.17
P_v	5.93	3.35	3.81	9.82	4.93	3.43	5.38	2.30	2.65
C_p	28.1	28.4	28.7	28.3	28.7	28.6	28.9	28.5	28.6

Table 1: Calculated QZ performance for each serration design.

As is almost ubiquitously used in industry and academia, for each of the simulated reflector models considered, typical QZ performance parameters have been derived which are listed in *Table 1*. Here, the labels f denotes frequency in GHz, A_v and P_v are the total amplitude- and phase-variation of the co-polar electric field inside the QZ, A_t is the amplitude taper, derived using a second order functional fit to the co-polar electrical field inside the QZ, A_r is the remaining variation after the amplitude taper has been subtracted from electrical field inside the QZ, and C_p is the maximum cross-polar level with respect to the normalized copolar level. A description of these parameters can be found in the open literature [1]. The cross-polar performance is shown largely for indicative purposes however it was not part of the optimization goal itself as this property is largely governed by the focal length of the parabolic reflector and the cross-polar performance of the feed, both of which were assumed fixed for the purposes of this study.

Table 1 suggests that the optimized serrations show improvements in both the amplitude and phase distributions. These improvements are also found in the co-polar plots shown in Figure 5 and Figure 6. Moreover, and upon careful examination of the amplitude behavior inside and outside the outlined QZ shown in Figure 5, one finds that the amplitude crosses the 1 dB level, which is often considered to mark the QZ limits, at ± 35 cm for the Genetic-optimized result, which is a more than 15% increase over the QZ diameter when compared with the cosine shaped serration which exhibited a ±30 cm limit. Furthermore, this very worthwhile increase in QZ size is gained with an overall reduction in ripple inside those limits which is a very desirable feature.

When, comparing the results at 12.5 GHz in Table 1, one might expect to see a better QZ amplitude performance for the cuts for the cosine shaped serration, however upon closer inspection it can be seen that the performance analysis algorithm overvalues the performance of a field distribution which shows, upon inspection, an almost flat amplitude taper, as is shown in Figure 7 below.

The current implemented algorithm takes approximately 0.5 seconds per child, and depending on the input parameter ranges an overall optimization takes about 2 hours.

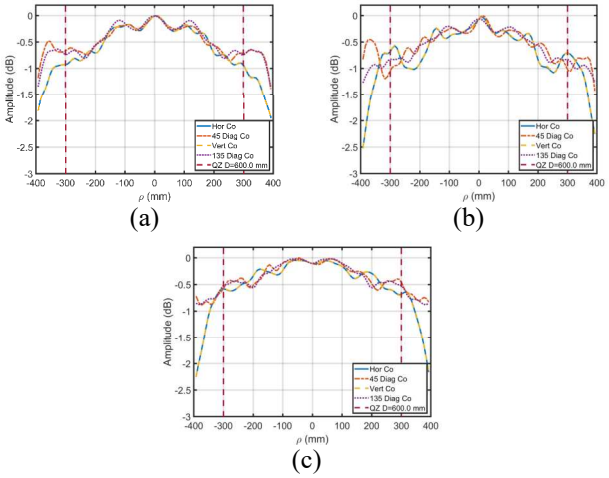

(a) (b)

(c)

Figure 5: Co-polar amplitude cuts through the QZ for (a) cosine, (b) circular-segmented and (c) Genetic-optimized, at 18 GHz

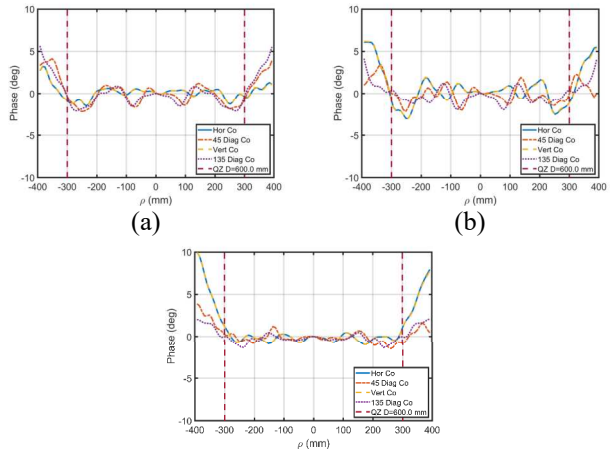

(a) (b)

(c)

Figure 6: Co-polar phase cuts through the QZ for (a) cosine, (b) circular-segmented and (c) Genetic-optimized, at 18 GHz

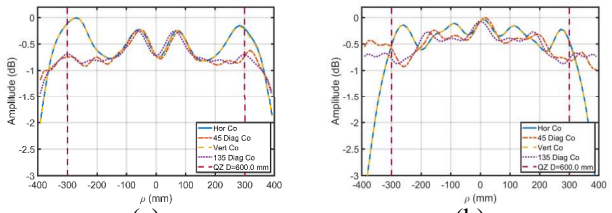

(a) (b)

Figure 7: Co-polar amplitude cuts through the QZ for (a) cosine, (b) Genetic-optimized, at 12.4 GHz

V. SUMMAY, CONCLUSION AND FUTURE WORK

The outline shape of the reflector serrations has been shown to have a significant impact on both the amplitude and phase behavior of the pseudo plane wave in the CATR QZ. Using the newly developed approach of combining the Superformula together with a genetic optimization algorithm, the QZ performance has been shown to have been significantly improved. Moreover, using this type of approach allows a CATR design to be specifically optimized for and adapted to a customer's specific requirements maximizing, amongst other things, the efficiency that chamber space is used. This is important to many customers, however it is of particular relevance to 5G FR2 test applications, especially those involving production test scenarios, where multiple test systems coexist within a single host building. Equally, it is clear that the demonstrated improvements allow, for fixed QZ dimensions, an overall reduction in facility size with a corresponding decrease in total cost of ownership.

This paper recounts the progress of an ongoing study and as such, a number of areas for future investigation are envisioned. One possible limitation of the current approach is that it is predicated on the assumption that the serration shape provides CATR performance that is inherently broadband in nature, with the optimization process being limited to the examination of a single chosen frequency. However, as this analysis can be readily expanded to operate across a band of frequencies by utilizing the extension a multi-objective genetic algorithm [15], this is an area that is intended for future investigation. Furthermore, as the optimized CATR performance can be combined with the authors preexisting 5G communications systems performance simulation capability, this optimization technique can be extended to provide facilities that are fully optimized for 5GNR testing.

REFERENCES

[1] C. Parini, S. Gregson, J. McCormick, D. Janse van Rensburg, T. Eibert, "Theory and Practice of Modern Antenna Range Measurements, 2nd Expanded Edition", Vol. 1, London: IET Press, 2020.

[2] E. Joy en E. Wilson, "Shaped Edge Serrations for Improved Compact Range Performance" in *AMTA Proceedings*, 1987.

[3] P. Beeckman, "Prediction of the Fresnel region field of a compact antenna test range with serrated edges," *Microwaves, Antennas and Propagation, IEE Proceedings H -,* vol. 133, pp. 108-114, 1986.

[4] M. Philippakis, C. Parini, "Compact antenna test range reflector edge treatment" *Electronic Letters,* vol. 32, nr. 2, pp. 82-83, 1996.

[5] W. Burnside, M. Gilreath, B. Kent en G. Clerici, "Curved Edge Modification of Compact Range Reflector" *Antennas and Propagation, IEEE Transactions on,* vol. 35, nr. 2, pp. 176-182, 1987.

[6] I. Gupta, K. Ericksen, W. Burnside, "A Method to Design Blended Rolled Edges for Compact Range Reflectors" *Antennas and Propagation, IEEE Transactions on,* vol. 39, nr. 6, pp. 853-861, 1990.

[7] T.-H. Lee, W. Burnside, "Compact Range Reflector Edge Treatment Impact on Antenna and Scattering Measurements" *Antennas and Propagation, IEEE Transactions on,* vol. 45, nr. 1, pp. 57-65, 1997.

[8] J. Hartmann, Grenzen, Störstrahlungs-unterdrückung bei der Vermessung von Mikrowellen, Millimeterwellenantennen in kompensierten Doppelspiegel-Compact-Range-Meßanlagen, München: Hieronymus, 2000.

[9] J. Hartmann en D. Fasold, "Improvement of compact ranges by design of optimized serrations," in *Millennium Conference on Antennas & Propagation (AP2000)*, Davos, Switzerland, 2000.

[10] K. Pontoppidan en P. Nielsen, "Guidelines for the Design of the Serrations of a Compact Range", *International Symposium on Antennas & Propagation (ISAP2000)*, Fukuoka, Japan, 2000.

[11] H. Schluper, "Verification Method for the Serration Design of CATR Reflectors" in *Amta Proceedings*, 1989.

[12] C. Schmidt, A. Geise, J. Migl, H.-J. Steiner, H.-H. Viskum, "A Detailed PO / PTD GRASP Simulation Model for Compensated Compact Range Analysis with Arbitrarily Shaped Serrations", *Antenna Measurement Techniques Association (AMTA)*, San Diego, California, 2013.

[13] J. Gielis, "Inventing the Circle, Antwerpen: Geniaal bvba", 2003.

[14] R. Dawkins, "The Blind Watchmaker 30th Anniversary Edition", Penguin, 2006.

[15] A. Eiben, J. Smith, "Introduction to Evolutionary Computing", Berlin: Springer-Verlag, 2015.